

## INFLUENCE OF SHADE ON SURFACE TEMPERATURE IN AN URBAN AREA ESTIMATED BY ASTER DATA

S. Kato<sup>a,\*</sup>, T. Matsunaga<sup>a</sup>, Y. Yamaguchi<sup>b</sup>

<sup>a</sup> Center for Global Environmental Research, National Institute for Environmental Studies, 16-2, Onogawa, Ibaraki, 305-8506, Japan - (kato.soushi, matsunag)<sup>a</sup>@nies.go.jp

<sup>b</sup> Graduate School of Environmental Studies, Nagoya University, D2-1(510), Furo-cho, Chikusa-ku, Nagoya, 464-8601, Japan - yasushi<sup>b</sup>@nagoya-u.jp

**KEY WORDS:** ASTER, Surface temperature, Shade, Vegetation, Impervious surface, Urban area

### ABSTRACT:

ASTER TIR data is useful to detect spatial distribution of surface temperature on wide area in high quality. According to surface temperature data around big cities from remote sensing, surface temperatures on urban centers are often lower than those on surrounding suburbs though urban heat island effect occurs in air temperature at near surface. Generally speaking, such patterns of surface temperature are caused by higher heat capacity of buildings, vegetation and water such as street trees, rivers and parks, and shadows of tall buildings. However, 90-m spatial resolution of ASTER TIR limits to analyze contribution of these factors because there are less pure pixels containing building, vegetation or shadow in urban areas. In this study, we tried to reveal the influences of material and condition of land surface to surface temperature data using ASTER data in Tokyo, Japan selected as a typical large city. First, we classified shade, vegetation and water body from ASTER VNIR data with 15-m spatial resolution, and estimated areal fraction of these surface categories in each pixel of TIR data on Tokyo in several seasons. Areal fractions of each surface type were compared with surface temperature in order to figure out influence of surface condition and material to surface temperature. The areal fraction of shade is up to 60% and up to 100% in spring and in winter, respectively, reflecting seasonal change of solar zenith angle. There was no clear relationship between vegetation fraction and surface temperature because surface temperature is less affected by area of vegetation than vegetation types. Areal fraction of water body also has no clear relationship with surface temperature since water temperature depends on depth as well as width of water body. On the other hand, shaded area affected surface temperature though there is not clear correlation between them. The deviation of surface temperature was smaller in the places with larger shaded fraction. The deviation of surface temperature is caused by surface coverage in sunlit areas. These results imply that shadow controls surface temperature equally in spite of the difference of surface coverage. Because surface temperatures in shaded areas are quite similar throughout a given scene, we estimated surface temperature in sunlit area in one pixel assuming the temperature is constant on shaded surface and long-wave radiation is proportional to the sunlit and shaded areal fractions. Surface temperatures on sunlit areas in mixed pixel around city center are as high as those on surrounding suburbs except for in winter. In winter time, estimated surface temperatures on sunlit areas are 5 to 10°C higher than those on suburbs because the assumption which this study applied inflates sunlit surface temperature unrealistically in the places with small sunlit ratios in one pixel. These results suggest that sunlit roofs in city center have higher surface temperature as much as those on residential areas, but the limitation of spatial resolution attenuates spatial pattern of surface temperature in urban areas on remote sensing data.

### 1. INTRODUCTION

In order to analyze thermal environment near land surface including urban areas, remote sensing data has been applied to heat balance analyses in wide areas. The authors have studied estimation of surface heat fluxes by using ASTER and the other satellite data (Kato and Yamaguchi, 2005; Kato and Yamaguchi, 2007; Kato et al., 2008). Though ASTER can observe surface temperature homogeneously in data quality and relatively higher accuracy throughout wide area, it is difficult to obtain detailed spatial pattern of surface temperature in urban area because the spatial resolution is 90m in Thermal Infrared (TIR) region of ASTER sensors. Because urban surface is constructed by several surface materials including natural and artificial one within small areas, we desire much higher spatial resolution to discern them. However, in the present thermal images from satellite remote sensing, the highest spatial resolution is 90m of ASTER and 60m of Landsat ETM+. According to TIR data from satellite sensors, surface temperatures in some urban centers are often lower than those in surrounding areas.

Generally speaking, such patterns of surface temperature are caused by higher heat capacity of buildings, vegetation and water such as rivers and parks, and shadows of tall buildings. However, abovementioned limitation of spatial resolution prevents to distinguish such influences. That is, lower and higher temperatures cancel each other in the mixed pixels.

Subpixel analyses of remote sensing data on urban areas has been attempted by choosing soil, water and impervious surface as endmembers in Visible and Near-infrared (VNIR) region and estimate their areal fraction in one pixel as Linear Spectral Mixture Analysis (LSMA) (for example, Ridd, 1995). Rashed (2001) used shadow as an additional endmember for LSMA because of the difference of urban fabric with Ridd (1995). Lu and Weng (2006) selected endmembers of hot- and cold-objects from TIR data and compared relationship between abundances of endmembers and surface temperature using correlation analysis from ASTER data. Although the study site is not urban area, spectral mixture analysis has been also applied for

---

\* Corresponding author.

multispectral thermal infrared data, but the purpose of these studies is to assess material fractions for geological survey using distinctive spectral emissivity of minerals eliminating temperature-related information (Gillespie, 1992). Other than selecting endmembers of typical surface materials in urban areas for LSMA, Tonooka (2005) enhanced ASTER TIR image using ASTER VNIR and Shortwave Infrared (SWIR) images based on spectral similarity of the same material.

In this study, the authors tried to detect subpixel temperature comparing TIR and VNIR data from ASTER. We take shade of buildings as one of key factors to control surface temperature in urban areas as well as water and vegetation. We analyzed relationships between surface temperature and areal fractions of shade, water and vegetation. After that, we estimated surface temperature on fractional sunlit surface in one pixel assuming that pixel of interest covers both sunlit and shaded areas.

## 2. DATA USED

We choose Tokyo, Japan as our study area because there are many tall buildings and wide roads; hence large shades appear on satellite images. Study area is shown in Figure 1. Selected study area is depend on an overwrapped area of ASTER images described below and roughly covers central part of Tokyo. Coverage area is about 430 km<sup>2</sup>.

Simultaneous pairs of ASTER level 2B03 (surface kinetic temperature) and 2B05 (surface spectral reflectance for VNIR region) products were used as satellite images with physical quantities. Spatial resolution of ASTER TIR data is 90m and is used as basis of this analysis. In order to compare seasonal difference, we used ASTER data taken on September 16, 2004 (autumn), December 14, 2007 (winter), January 17, 2009 (winter) and April 30, 2009 (spring). Elemental meteorological conditions are listed in Table 1. Solar zenith angle is included in metadata of ASTER data products. Air temperature was measured on meteorological observatory in Tokyo (35°41.3'N, 139°45.4'E) managed by Japan Meteorological Agency. Figure 2 shows spatial distributions of surface temperature from ASTER data for each day. Regardless of seasonal difference, surface temperature is smaller in central part of Tokyo. ASTER data taken in summer was eliminated from this analysis because smaller solar zenith angle makes shade of buildings smaller. All ASTER data products were provided by Earth Remote Sensing Data Analysis Center (ERSDAC), Japan.

As a reference map of water bodies in Tokyo, we used Detailed Digital Information (10m grid land use map) published by Geospatial Information Authority of Japan in 1994. Although there is a time interval more than 10 years between ASTER data used and the information for land use map, we assume that there are only small changes in shape of rivers and coastal lines.

	Solar zenith angle	Air temperature
Sep. 16, 2004	36.38 °	24.1 °C
Dec. 14, 2007	60.82 °	13.2 °C
Jan. 17, 2009	59.23 °	8.6 °C
Apr. 30, 2009	24.62 °	20.6 °C

Table 1. Elemental meteorological conditions of data acquisition dates

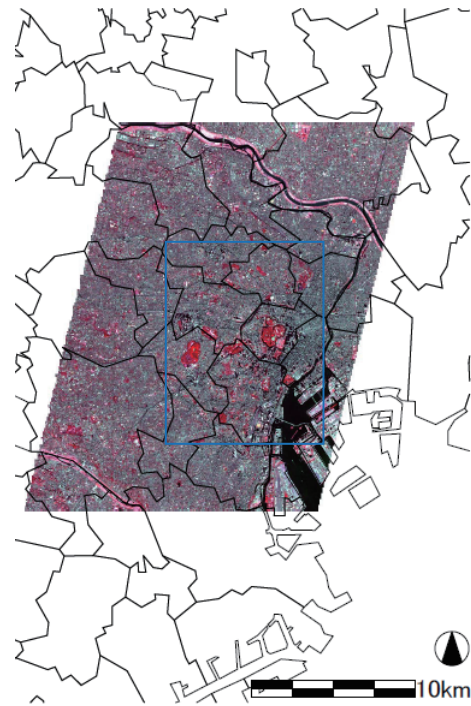


Figure 1. False colour image from ASTER VNIR data on January 17, 2009 showing study area

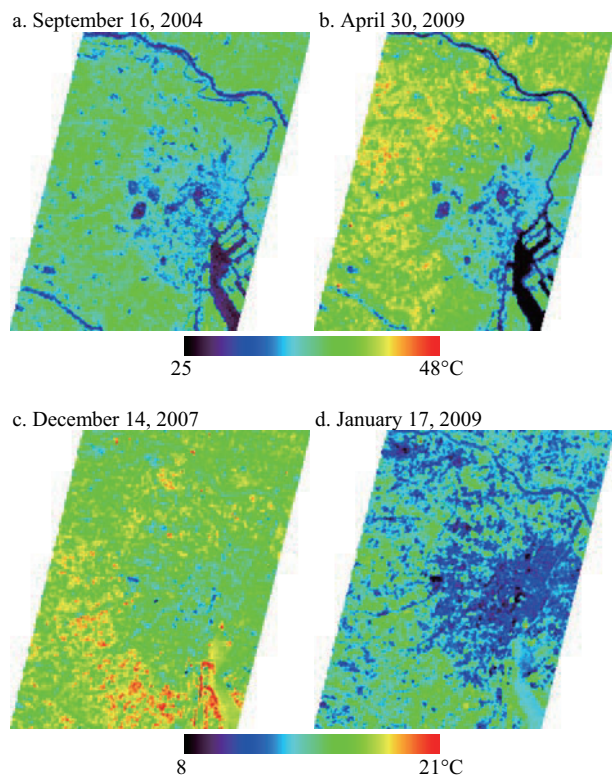


Figure 2. Spatial distributions of surface temperature

## 3. METHOD

In VNIR remote sensing, shaded areas are usually treated as useless data because VNIR sensors observe solar irradiance reflected at land surface. On the other hand, since TIR sensors

observe thermal radiance from land surface and inevitably atmosphere, TIR images contain information of surface temperature after applying appropriate atmospheric correction even if covered by shadow. In urban areas, shade as well as evapotranspiration by vegetation and water body limits temperature increase, in contrast with temperature increases on sunlit surface of bare soil and artificial material depending on their heat capacity. According to Meier et al. (2010), for instance, shadows affect long-wave radiation flux for day and night, which means that surface temperature remains lower on the temporally shadowed areas even after shadows disappeared. In this study, the authors tried to extract surface temperature on sunlit and shaded areas in one pixel of ASTER TIR data based on the thermal features of shadow, vegetation, water and the others. First, we analyzed the relationships between surface temperature and surface types especially shaded area.

Range of surface temperature can widely change according to constructions and materials of surfaces. In this study, the authors selected shade, vegetation and water body as the factors which control temperature increase in urban area. Hence we classified land cover as shade, vegetation, water and the others which are mostly impervious surface, using ASTER VNIR data. We extracted shaded areas by setting thresholds for VNIR bands 1, 2 and 3 manually according to their relatively lower spectral reflectance on shaded areas. In fact lower reflectance is apparent value because solar radiation is blocked out by surrounding buildings. However, large water bodies can be misclassified as shaded area because of their similarity of spectral reflectance. We corrected such misclassification by masking the areas coded as "river and lake" and "sea" in Detailed Digital Information (10m grid land use map) assuming change in spatial distribution of water bodies is small in spite of seasonal difference. Vegetation was classified from remaining areas using empirical thresholds for Normalized Difference Vegetation Index (NDVI) which was estimated from bands 2 and 3 of VNIR data. The authors avoid applying popular supervised classification methods, e.g. maximum likelihood and minimum distance procedure, because these classification techniques strongly depend on selection of training areas and the target categories, namely shade and vegetation, have significant spectral patterns which can be detected even from manual thresholds on DN values. Unsupervised classification methods are also avoided because we just need mere three categories.

Based on the difference of spatial resolution between VNIR (15m) and TIR (90m) data, we estimated areal fractions of shade, vegetation and water in each TIR pixel.

## 4. RESULTS

### 4.1 Spatial Patterns of Areal Fractions

Areal fractions of shade, vegetation and water body are shown in Figure 3. Since each areal fraction clusters in the same places for all seasons, these surface categories were extracted well. Obvious seasonal difference appeared on the spatial distribution of shaded fraction. In spring and autumn, shaded areas are smaller than winter time because of smaller solar zenith angles in these seasons. In Tokyo, tall buildings are concentrated around train terminals and stations. The largest shaded fraction was about 60% in spring and autumn, and 100% in winter, respectively, near Tokyo terminal and Shinjuku station where some buildings are taller than 200m. In winter, shaded fraction

reached about 50% along highways because of the vertical intervals between highways, roads beneath and surrounding buildings. Meanwhile shaded fraction was mere about 10% along highways in spring and autumn.

Water fraction shows the same pattern for all seasons because it is based on one land use map. In the city center, seasonal change of vegetation fraction roughly depends on distribution of deciduous and evergreen trees, namely more deciduous trees show smaller vegetation fraction in winter though vegetation fraction has small seasonal change, because most of vegetation exist in parks and as street trees. Moreover, vegetation fraction is 100% for all seasons because of dense evergreen trees in some parks. On the other hand, vegetation fraction is slightly smaller in winter in surrounding suburbs and along riversides. These seasonal changes are caused by annual phenological cycle and/or trimming of grass plants and agricultural activities. Agricultural area occupies about 1.7% of central part of Tokyo, for reference.

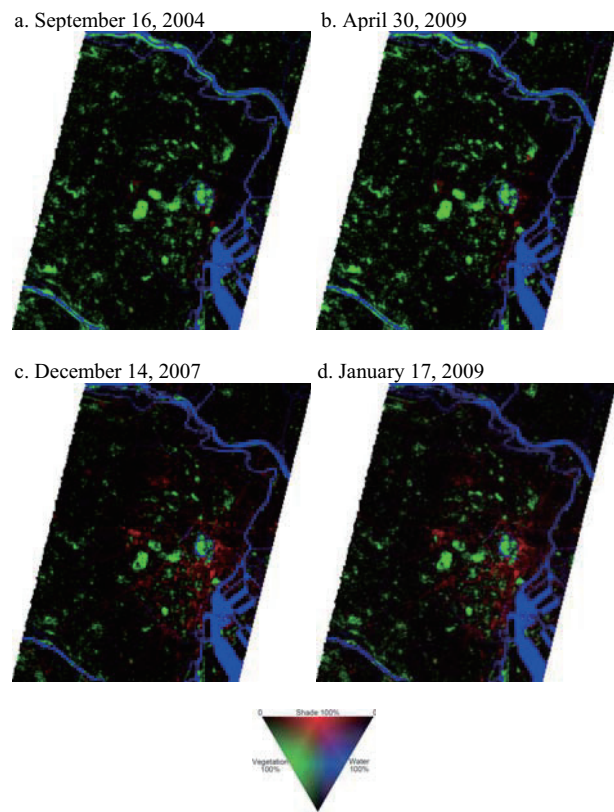


Figure 3. Areal fraction for shade, vegetation and water body

### 4.2 Relationship between Areal Fractions and Surface Temperature

Scatter plots between areal fractions and surface temperature are shown in Figure 4. There is no correlation between these two parameters. However, the scatter plots show characteristic triangle shape, namely, smaller temperature range in larger shaded fraction. Range of surface temperature is about 20°C, 30°C and 10°C in autumn, spring and winter, respectively, when the shaded fraction is smallest (2.8% = 1/36 pixels), and is linear dependence with solar zenith angle. Air temperature has no linear relationship with range of shaded fraction and solar zenith angle because air temperature depends not only on

surface heat balance but also on atmospheric condition such as relative humidity, wind speed and wind direction. These results imply that temperature difference mainly depends on evapotranspiration and thermal properties of sunlit surfaces, in other words, surface temperature on shaded areas are similar in spite of difference in land cover type.

In contrast, ranges of surface temperature have no relation with areal fraction of vegetation and water body. The authors assume that this result is because areal fraction indicates not bulk but footprint of objects. Surface temperature primarily depends on evapotranspiration in vegetation and water body. Transpiration occurs from leaf surface and vegetations have heights. Moreover, transpiration efficiency is different according to vegetation types. In case of water body, surface temperature kept lower on wider and/or deeper water body in daytime because of larger specific heat of water, in addition to evaporation. However, because remote sensing cannot capture vegetation type and the vertical structure of features, or volumes of vegetation and water body, areal fraction is an inadequate index for vegetation and water areas.

In winter time, the lowest temperature on shaded areas is lower than air temperature despite the value of shaded fraction. On the other hand, the lowest surface temperature exceeds air temperature in autumn and spring. Hence, air temperature cannot be substitution of temperature on shaded surface.

temperature on shaded areas in particular scene. We estimated surface temperature on sunlit surface based on additional following assumptions: broadband longwave radiation is proportional to area, and surface emissivity is homogeneous in subpixel level. From these assumptions, surface temperature on sunlit surface can be estimated by equation (1) based on Stephan-Boltzmann law.

$$T_{sunlit} = \left( \frac{T_0^4 - a_{shade} T_{shade}^4}{1.0 - a_{shade}} \right)^{1/4} \quad (1)$$

where  $T_{sunlit}$  = surface temperature on sunlit surface  
 $T_{shade}$  = surface temperature on shaded surface  
 $T_0$  = surface temperature from ASTER data  
 $a_{shade}$  = shaded fraction (0 - 1)

We used minimum surface temperature with 100% of shaded fraction as  $T_{shade}$ . Figure 5 compares spatial distributions of actual and hypothetical sunlit-only surface temperatures around Tokyo central area. In general, both patterns of surface temperatures are quite similar because sunlit surface temperature substitutes actual one on the pixels with shaded fraction > 0% which occupies 3.8%, 21.2%, 23.6% and 7.1% of whole study area on September 16, 2004, December 14, 2007, January 17, 2009 and April 30, 2009, respectively. In spring and autumn, values of sunlit surface temperatures are comparable with surface temperatures in surrounding suburbs. Temperatures on sunlit surface are at most 15°C and 10°C higher, approximately, than surface temperature of 90m resolution in spring and autumn, respectively. On the other hand, sunlit surface temperatures are 5 to 10°C higher than the surrounding suburbs and factories in winter. Because roofs of factories are wide and homogeneous, longwave radiation from them can be comparable with longwave radiation from sunlit surface. Hence we consider that such a high temperature on sunlit surface is unrealistic result. Moreover, temperatures on sunlit surface are more than 20°C higher than the original pixel values on the places with relatively high surface temperature and more than 78% of shaded fraction. In such condition, equation (1) results in extremely high temperature caused by combination of small denominator and large numerator. Shaded fraction might be overestimated caused by 15m of spatial resolution for ASTER VNIR. Meanwhile McCabe et al. (2008) simulated the estimation error arose retrieving thermal infrared temperature using Planck's function from spectral radiance. According to their results, difference between the mean temperature of the subpixels and the ensemble temperature retrieved from the mean radiance is less than 10°C when the subpixel temperature difference is 40°C. Although both the methodology and assumption are different, similar effect can occur in this study. ASTER kinetic temperature product was retrieved from the ASTER Temperature Emissivity Separation (TES) algorithm which estimates surface temperature and spectral emissivities from Planck's function using empirical minimum emissivity (Gillespie et al., 1998). In this study, based on surface temperature retrieved by this procedure, surface temperature on sunlit surface is estimated by equation (1), in other words Stephan-Boltzmann law. Thus the difference of these methods, though theoretically comparable, can affect the accuracy of retrieved surface temperature.

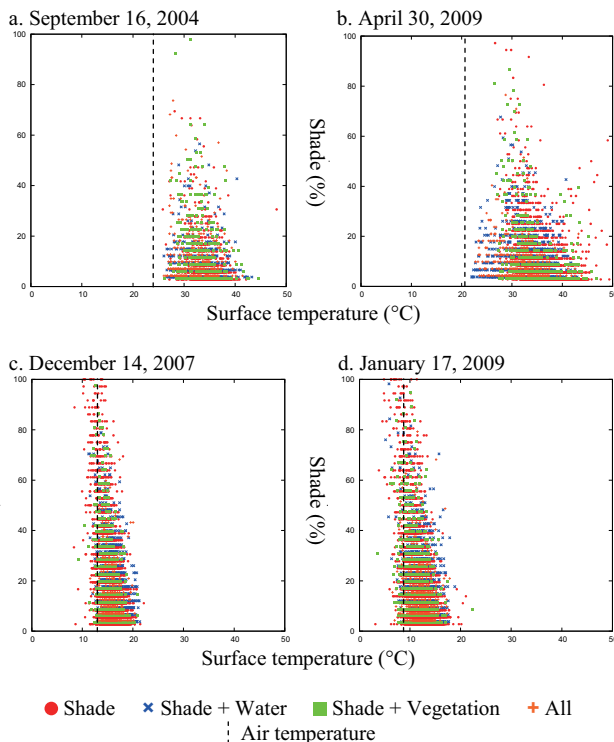


Figure 4. Scatterplots between shaded fraction and surface temperature

### 4.3 Inference of Surface Temperature on Shaded Surface

As discussed in 4.2, values of surface temperature are similar on shaded surface in spite of land cover type. Thus we tried to infer surface temperature on sunlit surface in sunlit/shaded mixed pixels simply assuming constant value of surface

a. September 16, 2004

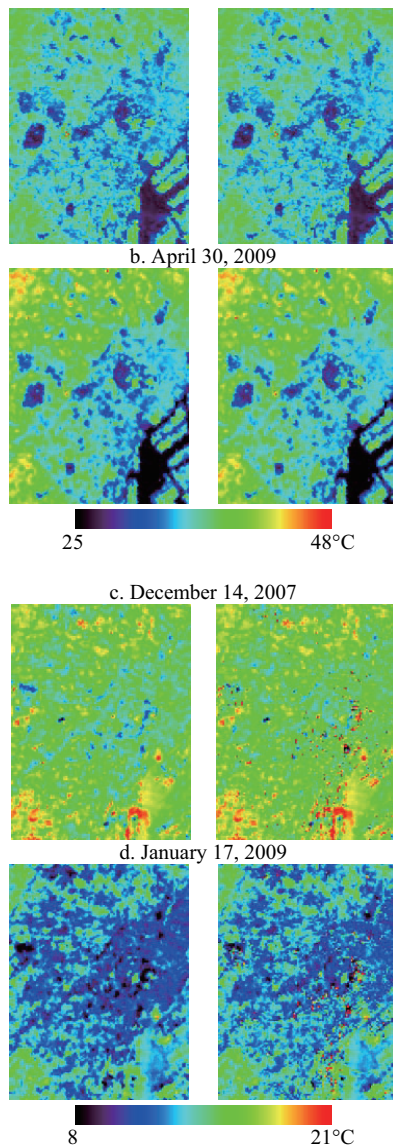


Figure 5. Surface temperature from ASTER data (left) and on sunlit surface (right). Location is shown in Figure 1.

## 5. CONCLUSION

This study estimate areal fraction of shade in Tokyo, Japan and its effect to surface temperature from ASTER. There is obvious characteristic relationship between shaded fraction and surface temperature in comparison with vegetation and water body. Because of smaller temperature range on shaded surface, surface temperature on sunlit area was inferred assuming surface temperature on shaded area are the same regardless of land cover type. Shaded/sunlit temperature difference appears on limited areas because shaded area occupies small portion of study area even in winter. Surface temperature on sunlit surface is comparable with surface temperature on suburbs in spring and autumn, but can be overestimated in winter. In this stage, the procedure to infer surface temperature on sunlit surface contains considerable error because of its simplified assumptions. Moreover, spatial resolution of ASTER (15m) can result in considerable over- or underestimation of shaded fraction. However, the shaded places are extracted well visually. Largely shaded places result in especially lower surface

temperature in winter. As a whole, spatial distribution of sunlit surface temperature is similar with that of ASTER surface temperature product. This result implies that extensive vegetation and water and higher heat capacity of buildings have larger influence to lower surface temperature in urban center. In the future study, we would like to distinguish influences by evapotranspiration, heat capacity and shade to thermal environment in urban area estimating sunlit/shaded surface temperature more accurately.

## References

- Gillespie, A. R., 1992. Spectral mixture analysis of multispectral thermal infrared images. *Remote Sensing of Environment*, 42(2), pp. 137-145.
- Gillespie, A., Rokugawa, S., Matsunaga, T., Cothorn, J. S., Hook, S. and Kahle, A. B., 1998. A temperature and emissivity separation algorithm for Advanced Spaceborne Thermal Emission and Reflection Radiometer. *IEEE Transactions on Geoscience and Remote Sensing*, 36(4), pp. 1113-1126.
- Kato, S. and Yamaguchi, Y., 2005. Analysis of urban heat-island effect using ASTER and ETM+ data: Separation of anthropogenic heat discharge and natural heat radiation from sensible heat flux. *Remote Sensing of Environment*, 99(1-2), pp. 44-54.
- Kato, S. and Yamaguchi, Y., 2007. Estimation of storage heat flux in an urban area using ASTER data. *Remote Sensing of Environment*, 110(1), pp. 1-17.
- Kato, S., Yamaguchi, Y., Liu, C.-C. and Sun, C.-Y., 2008. Surface heat balance analysis of Tainan City on March 6, 2001 using ASTER and Formosat-2 data. *Sensors*, 8(9), pp. 6026-6044.
- Lu, D. and Weng, Q., 2006. Spatial mixture analysis of ASTER images for examining the relationship between urban thermal features and biophysical descriptors in Indianapolis, Indiana, USA. *Remote Sensing of Environment*, 104(2), pp. 157-167.
- McCabe, M. F., Balick, L. M., Theiler, J., Gillespie, A. R. and Mushkin, A., 2008. Linear mixing in thermal infrared temperature retrieval. *International Journal of Remote Sensing*, 29(17-18), pp. 5047-5061.
- Meier, F., Scherer, D. and Richters, J., 2010. Determination of persistence effects in spatio-temporal patterns of upward long-wave radiation flux density from an urban courtyard by means of Time-Sequential Thermography. *Remote Sensing of Environment*, 114(1), 21-34.
- Rashed, T., Weeks, J. R. and Gadalla, M. S., 2001. Revealing the anatomy of cities through spectral mixture analysis of multispectral satellite imagery: a case study of the Greater Cairo region, Egypt. *Geocarto International*, 16(4), pp.5-16.
- Ridd, M. K., 1995. Exploring a V-I-S (vegetation-impervious surface-soil) model for urban ecosystem analysis through remote sensing: comparative anatomy for cities. *International Journal of Remote Sensing*, 16(12), pp. 2165-2185.
- Tonooka, H., 2005. Resolution enhancement of ASTER shortwave and thermal infrared bands based on spectral similarity. *Proceeding of SPIE*, 5657, pp. 9-19.